A GEOSPATIAL ANALYSIS OF THE

URBAN HEAT ISLAND EFFECT IN AUSTIN, TX

HONORS THESIS

Presented to the Honors Committee of
Texas State University
in Partial Fulfillment
of the Requirements

for Graduation in the Honors College

by

Shae Mackenzie Richardson

San Marcos, Texas
May 2015

A GEOSPATIAL ANALYSIS OF THE

URBAN HEAT ISLAND EFFECT IN AUSTIN, TX

Thesis Supervisor:

_____

Jennifer Jensen, Ph.D.
Department of Geography

Second Reader:

_____

Matthew Lewis, B.S.
City of Austin, Planning and Development

Approved:

_____

Heather C. Galloway, Ph.D.
Dean, Honors College

ACKNOWLEDGEMENTS

I would never have been able to finish my thesis without the guidance of my committee members and the support from my family and friends.

I would like to express my sincere gratitude to my supervisor, Dr. Jennifer Jensen, for the continuous support of my thesis and analysis. For her sharing her immense knowledge, patience, and motivation.

My sincere thanks also goes to my second reader, Mr. Matthew Lewis, for his infinite enthusiasm, guidance, and encouragement.

Lastly, I am grateful to my wonderful parents, siblings, and boyfriend, for never letting me give up and standing by my side throughout my entire undergraduate career.

TABLE OF CONTENTS

LIST OF FIGURES

Figure Page

LIST OF TABLES

LIST OF EQUATIONS

Equations Page

ABSTRACT

Over the past 30 years, Central Texas has become a highly desirable location to live, resulting in Austin being one of the fastest growing cities in the United States. Given the rapid population growth and associated development of Austin and surrounding suburbs, the region provides a good case study to analyze the Surface Urban Heat Island (SUHI) using thermal remote sensing data. The increase in population is logically correlated to an increase of urban development, which is a contributing factor of UHIs. Since UHIs negatively impact people's health and the environment, monitoring UHIs is of critical importance. The focus of this study will be to determine if land surface temperatures (LST) have increased in Austin, Texas between 1993 and 2011 and whether land cover type influences surface temperature. Although the existing literature has demonstrated the connections between land cover type and surface temperature for selected cities, an analysis of the Austin, Texas metropolitan area has not been conducted. Therefore, methods drawn from previously performed analysis were utilized to develop a framework for geospatial analysis of surface temperatures in Austin. Results indicate the presence of the UHI effect. Results show that the average surface temperature for Austin increased by 4.7 degrees C between 1993 to 2011. The largest temperature increases occurred for developed, barren, and cultivated land class.

1.0 INTRODUCTION

An Urban Heat Island (UHI) is defined as an urban area having higher average surface temperatures than its rural surroundings (Climatology 2nd ed., 8). UHIs result from greater absorption, retention, and production of heat due to urban infrastructure and human activities (Climatology 2nd ed., 8) They are an important issue because of the negative effects on the environment and human beings. These include decreased air and water quality, increased occurrence of heat waves, and corresponding increases in mortality rates, particularly among young children and the elderly (EPA.gov, Impacts, 2013).

Urban heat islands are caused by numerous variables. The main cause can be attributed to the modification of land surfaces through urban development, which uses materials that effectively retain heat. For example, the building of structures that remove vegetation from the landscape effectively blocks surface heat from radiating into the relatively cooler night sky (dallastrees.org). Land cover types that contribute to increased heat retention include pavement, rooftops, sidewalks, roads, and parking lots. In addition to specific surface types, the color and composition of the material plays an important role as well. For example, darker materials such as black asphalt have non-evaporative and nonporous properties, and therefore tend to have a low albedo (percent of solar reflectance); ranging from 5 to 40 percent. These low albedo surfaces absorb and retain far greater amounts of heat than natural environments at about 95-60 percent energy absorption (epa.gov, Cool Pavements, 2005), while natural, lighter colored materials have a much higher albedo providing for significantly less heat absorption. Overall, low albedo, high-energy absorption surfaces contributed considerably to increased surface

temperatures (epa.gov, Cool Pavements, 2005). To exacerbate the problem, waste heat from air conditioners and cars also contributes additional heat to the local environment and continues to do so in times when nighttime cooling should occur (Climatology 2nd ed., 49). According to the U.S. Environmental Protection Agency, the UHI effect has the ability to increase average air/surface temperatures in large cities up to 5.6 degrees C warmer than the surrounding rural areas (ucar.edu, Urban Heat Islands, 2011).

Another significant health effect caused by UHIs is an overall decrease in air quality (EPA.gov, Impacts, 2013). Air conditioners, cars, and refrigerators contribute to the increase of air pollutants as well as the increase in greenhouse gas emissions, which greatly compromises the overall air quality within a city (EPA.gov, Impacts, 2013). Greenhouse gasses (GHG) including carbon dioxide (CO_2), water vapor, and methane are responsible for significant energy retention, due to their ability to absorb short and long wave radiation (energy) and further obstruct energy transmission from the Earth's surface back to space. Thus, the energy absorbed by GHG is either retained or re-emitted back to Earth's surface, resulting in warmer air temperatures compared to undeveloped areas (Climatology 2nd ed., 286).

Additionally, UHIs have great potential to increase the magnitude and duration of heat waves within cities, which correspondingly increases heat-related illnesses and mortality rates (EPA.gov, Impacts, 2013). Just within the United States, an average of 1,000 people die each year due to extreme heat conditions (EPA.gov, Impacts, 2013). The increased surface temperatures corresponding to UHIs result in an increase in overall physical discomfort, respiratory difficulties, heat cramps, heat exhaustion, strokes, and heat related deaths (EPA.gov, Impacts, 2013). Children and elderly people are at greater

risk of these heat-related threats, especially those with existing heart or respiratory health conditions. The Centers for Disease Control and Prevention (CDC) published a study in 2009 that reported excessive heat exposure was the cause of 8,015 premature deaths in the United States between 1979 and 2003 (Extreme Heat Prevention Guide Pt.1, CDC, 2009). The CDC also discovered that during that time, heat-related deaths exceeded the amount of deaths caused by hurricanes, tornadoes, lightning, earthquakes, and floods combined (Extreme Heat Prevention Guide Pt.1, CDC, 2009).

Urban heat islands can be characterized in two ways: atmospheric and surface heat islands (Stathopoulou & Cartalis, 2006). Atmospheric heat islands include the urban canopy layer (UCL) and the urban boundary layer (UBL). Atmospheric UHIs are best distinguished on calm clear nights and are typically found by air temperature measurements that are ground-based (e.g. taken from standard meteorological stations) (Voogt & Oke, 2003).

The surface urban heat island (SUHI) is described as the areas of relative warmth, where increased temperatures are a result of urban surfaces compared to the surrounding rural surfaces (Oke, 1976). SUHIs are most noticeable during the day, when urban heat intensity is greatest, and are typically measured by thermal remote sensors (Voogt et al., 2003). Thermal remote sensors are non-contact instruments, which record emitted thermal infrared (TIR) radiation, enabling an estimate of the surface temperatures (Voogt et al., 2003). This analysis will be concentrated on SUHIs; therefore, thermal remote sensing will be used to characterize a SUHI.

1.1 BACKGROUND

1.1.1 Population growth and urban development in Central Texas

Over the past 30 years Central Texas has become a highly desirable location to live. Whether it's for the beautiful hill country, low cost of living, delicious food, booming job market, respected film industry, or for holding the musical capital of the US, Central Texas has something for everyone (realtyaustin.com). All of which, are contributing factors as to why so many people are moving to this region. For the past four years, Austin, Texas has been listed at number one on Forbes list of Top 20 fastest growing cities (Carlyle, 2014). In 2013, Austin exhibited a 2.5 percent population growth rate and an economic expansion of 5.88 percent (Carlyle, 2014). As of 2015, Austin has a population of 900,701. According to Robinson (2015), the population of Austin is projected to increase within the next 30 years to approximately 1.3 million people. Given this rapid population growth, urban and exurban areas are expected to expand as well.

1.1.2 Characteristics of remotely sensed data with Landsat as a specific example

Although there are hundreds of remote sensing instruments orbiting the Earth, a specific platform that has been used successfully to characterize and monitor SUHIs is the Landsat series of sensors. With the first Landsat satellite launched in 1972, the Landsat program is the oldest land-surface observation satellite system in the United States (Jensen, 2007, 197). Landsat is a joint program between National Aeronautics and Space Administration (NASA) and the U.S. Geological Survey (USGS) with a mission to

provide essential information to assist land managers and policy makers in natural resource and environmental decision-making (nasa.gov, Landsat Science, 2015).

Selecting the right satellite data to use in an analysis requires an analyst to consider the various resolution characteristics of the sensor. Resolution can be characterized four different ways: spatial, spectral, radiometric, and temporal. Spatial resolution refers to the smallest angular or linear separation between two objects. In simple terms, spatial resolution corresponds to the real-world area on the Earth's surface that is represented by each picture element ("pixel"). The size of an individual pixel in a particular satellite image is used to convey the spatial resolution of that sensor (e.g., 5 m x 5 m). Spectral resolution refers to the number of bands in a satellite image. Remote sensors can detect specific wavelength intervals of the electromagnetic spectrum (EMS) and store that information as individual layers (i.e., blue, green, red, and near-infrared).

Radiometric resolution is defined as the sensitivity of the sensor's detectors to variations in energy reflected or emitted from the Earth's surface. Sensors with a high radiometric resolution (e.g. 16-bit) can record slight variations in energy received at the detectors, while sensors with a lower radiometric resolution (e.g. 8-bit) can only record large variations. Finally, temporal resolution refers to how frequently a sensor acquires imagery over the same area on the Earth's surface (Jensen, 17). The Landsat series of sensors exhibit a range of sensor resolutions depending on the particular instrument. Refer to Table 1 for a summary of each sensor's resolution characteristics. Given the relatively fine spatial resolution of the Landsat 5 and Landsat 8 thermal bands, as well as the 16-day temporal resolution, Landsat data are a valuable resource to use in SUHI analyses.

Table 1: Resolution characteristics of individual Landsat sensors

Sensors	**Landsat**	**Resolution (meters)**	**Spectral Bands**
Multispectral Scanner (MSS)	1-3 & 4-5	30	B, G, R, NIR
Thematic Mapper (TM)	4-5	30	B, G, R, NIR, SWIR, TIR
Enhanced Thematic Mapper Plus (ETM+)	7	30, Pan (15)	B, G, R, NIR, SWIR, TIR, PAN
Operational Land Imager (OLI) and Thermal Infrared Sensor (TIRS)	8	30, Pan (15)	B, G, R, NIR, SWIR, TIR, PAN

Source: http://landsat.usgs.gov/band_designations_landsat_satellites.php

1.2 Problem Statement:

Since Austin is one of the fastest growing cities in the United States, it provides a good case study to analyze a SUHI using thermal remote sensing data. As previously stated, the increase in population is logically correlated to an increase of urban development, which is also a contributing factor of UHIs. Given that UHIs affect people's health and the environment, monitoring UHIs is of critical importance. The focus of this study will be to determine if land surface temperatures have increased over the years in relation to population growth and increased urban expansion in Austin, Texas.

1.3 Research Questions:

1. Have land surface temperatures (LST) increased in Austin, Texas between 1993 and 2011?
2. Does land cover type influence LST?

1.4 Justification:

Although the existing literature has demonstrated the connections between land cover type and surface temperature for selected cities, an analysis of the Austin, Texas metropolitan area has not been conducted. Therefore, by using a combination of thermal remote sensing data from the U.S. Geologic Survey (USGS) and spatially analyzing land cover data in ArcMap software has not yet been performed. The various negative impacts on human health and the environment make this issue a significant and widespread concern. Fortunately, this method is not limited to Austin, enabling a wide range of interest to anyone living in a highly populated area with increasing urban development.

2.0 LITERATURE REVIEW

Several studies have examined the utility of remotely sensed thermal infrared data to characterize and monitor the UHI effect. For example, Stathopoulou and Cartalis (2006) presented a study of the thermal environments in five major cities in Greece: Athens, Thessaloniki, Patra, Volos, and Heraklion. They used Landsat Enhanced Thematic Mapper (ETM+) acquired for five dates of imagery during the months of May to August in years 2000 and 2001, to determine temperature differences in rural versus urban areas. Their analysis identified the hottest surfaces within the urban areas and examined the spatial relationship of surface temperature with land use characteristics available from the Corine land cover (CLC) data published by the European Environment Agency. Their results demonstrated that urban areas within each of the cities exhibited

higher surface temperatures compared to non-urban areas. For instance, central Athens was 3.3 degrees C warmer and suburban areas were 2.3 degrees C warmer than the surrounding undeveloped areas. They also noted presence of hot spots in mixed urban areas of the city, with temperatures 5.2 degrees C warmer than undeveloped areas, which they attributed to asphalt and concrete surfaces as well as solar heating of open spaces with bare soil due to mines and dumpsites.

Another study by Lo, Quattrochi, and Luvall (1996) examined differences in daytime versus nighttime thermal temperatures of urban land cover types in Huntsville, Alabama for September 7, 1994. They used 5 m thermal infrared data collected by the Advanced Thermal and Land Applications Sensor (ATLAS) airborne sensor. In addition to the land cover-temperature comparisons, they examined the relationship between surface temperature and vegetation density as measured by the Normalized Difference Vegetation Index (NDVI). Using simple GIS analysis, they found that for 351 observation sites, a strong negative correlation between the surface temperature and NDVI. In other words, surface temperatures were lower, for both daytime and nighttime observations for land cover types that had a significant amount of vegetation cover.

In 2008, Mallick, Kant, and Bharath (2008) published a study that focused on characterizing surface temperatures for Delhi, India. Using Landsat 7 EMT+ data, they classified the imagery in to specific land cover types, NDVI, and fractional vegetation cover (FVC) and compared those products to satellite-derived and field measured surface temperatures. They reported that surface temperatures derived from Landsat

corresponded well with field-measured temperatures and that stong and moderate correlative relationships existed between land surface temperatures and NDVI and FVC, respectively. Based on those results, they developed a regression model that accurately predicted land surface temperatures based on NDVI values.

Finally, Imoff et al. (2009) performed a spatial analysis across biomes in the continental USA over three annual cycles (2003-2005) of impervious surface area (ISA) data from the USGS 2001 National Land Cover Data (NLCD) as well as LST data from the Moderate Resolution Imaging Spectroradiometer (MODIS) sensor. The researchers determined that ecological context considerably influenced the amplitude of daytime summer UHI temperature differences between urban and rural land covers. The largest difference was between cover types was an average of 8 degrees C. This difference involved the cities that were developed in areas dominated by broadleaf and mixed forest biomes. Combining all cities, 70 percent of the total variance in LST temperature increase was primarily driven by ISA. Urban areas were found to be an annual average of 2.9 degrees C warmer than rural surroundings, excluding urban areas in biomes with arid/semiarid climates. These observations concluded that the magnitude of UHIs both increases with city size and is seasonally unbalanced for a large number of cities throughout various biomes.

Although the existing literature has demonstrated the connections between land cover type and surface temperature for selected cities, an analysis of the Austin, Texas metropolitan area has not been conducted. Therefore, I will draw from the methods

described above to develop a framework for the geospatial analysis of surface temperatures in Austin as they relate to land cover type and spatial proximity to highly developed areas within the city.

3.0. MATERIALS AND METHODS

3.1 Data Collection

Four Landsat 5 TM images were downloaded from USGS Earth Explorer (http://earthexplorer.usgs.gov) for two summer dates in both 1993 and 2011. Refer to Table 2 for a summary of the specific image dates. Dates chosen for Landsat data were based on the best available images, namely image dates that were available in the summer and had the least amount of cloud cover. Less cloud cover allows for more accurate determination of surface temperatures since clouds obscure the land surface. Additional data consists of two sets of National Land Cover Data (NLCD) from the USGS. NLCD data from1992 and 2011 were downloaded from the Multi-Resolution Lands Characteristic Consortium (MRLC) website (http://www.mrlc.gov/index.php). To clip the Landsat and NLCD data, a shapefile of the City of Austin was downloaded from the Texas Natural Resource Information System (TNRIS; https://tnris.org).

Table 2: Image dates for Landsat data: http://earthexplorer.usgs.gov

Year	Month	Day	TM-Landsat	Band (thermal)	Resolution (m)	Cloud Cover (%)
1993	July	23	5	6	30	0
	August	8	5	6	30	10
2011	July	25	5	6	30	6.42
	August	10	5	6	30	12.59

3.2 Data Processing

Spatial analysis is useful for geographic research as it enables the analyst to extract or create new information as well as to acquire important information concerning spatial relationships, differences or interactions, between geographic events (A to Z GIS, ESRI, 2006). All data were organized, managed, and analyzed using ArcGIS (ESRI, Redlands, CA). Each layer of data was compiled and projected into the World Geodetic System 1984 (WGS84) datum and the Universal Transverse Mercator (UTM) coordinate system.

3.2.1 TM-Landsat 5 Imagery

Each Landsat thermal band for the four image dates was clipped to Austin's boundary layer using the spatial analysis tool, Extract by Mask. After the extraction, raw digital numbers were first converted into spectral radiance (L_λ) and then to at-sensor temperature in Kelvin. Kelvin temperatures were then converted to degrees Celsius. Conversions were implemented using the raster calculator tool in Model Builder using the following equations:

$$L_\lambda = G_{rescale} \times Q_{cal} + B_{rescale} \qquad \text{(Equation 1)}$$

L_λ = Spectral radiance at the sensor's aperture [$W/(m^2\ sr\ \mu m)$]

Q_{cal} = Quantized calibrated pixel [DN] (raster values)

$G_{rescale}$ = Band specific rescaling gain factor [$(W/(m^2\ sr\ \mu m))/DN$]

$B_{rescale}$ = Band-specific rescaling bias factor [$W/(m^2\ sr\ \mu m)$]

$$T = \frac{K2}{\ln\left(\frac{K1}{L\lambda}+1\right)}$$ (Equation 2)

T = Effective at-sensor brightness temperature [K]

K2 = Calibration constant 2 [K]

K1 = Calibration constant 1 [W/(m^2 sr μm)]

L_λ = Spectral radiance at the sensor's aperture [W/(m^2 sr μm)]

ln = Natural logarithm

After conversion to at-sensor temperature, the average surface temperatures for each year were calculated as well as the temperature difference between 1993 and 2011.

3.2.2 National Land Cover Data

Both NLCD sets were also clipped to Austin's City boundary using the Extract by Mask tool. The NLCD represents a set of land cover classification types. Land cover data for 1992 consists of 21 different classes while 2011 land cover data consist of 20 different types. For the purpose of this analysis, each year's classification was reclassified and simplified to represent 11 broad classifications (1992: Table 3, 2011: Table 4). Developed areas were split into four levels of open space, low, medium, and high intensity. This allowed for a more detailed classification and better understanding of the areas that are of high development.

Table 3: Reclassification table for NLCD 1992

11	Open Water
12	Perennial Ice/Snow
85	Urban/Recreational Grasses
21	Low Intensity Residential
22	High Intensity Residential
23	Commercial/Industrial/Transport
31	Barren Land
32	Gravel Pits
33	Transitional Barren
41	Deciduous Forest
42	Evergreen Forest
43	Mixed Forest
51	Shrubland
71	Grassland/Herbaceous
81	Pasture Hay
82	Row Crops
83	Small Grains
84	Fallow
90	Woody Wetlands
95	Emergent Wetlands

10	Water
21	Developed, Open Space
22	Developed, Low Intensity
23	Developed, Medium Intensity
24	Developed, High Intensity
30	Barren
40	Forest
50	Shrub
70	Herbaceous
80	Cultivated
90	Wetlands

Table 4: Reclassification table for NLCD 2011

11	Open Water
12	Perennial Ice/Snow
21	Developed, Open Space
22	Developed, Low Intensity
23	Developed, Medium Intensity
24	Developed, High Intensity
31	Barren Land
41	Deciduous Forest
42	Evergreen Forest
43	Mixed Forest
51	Dwarf Shrub (Alaska Only)
52	Shrub/Scrub
71	Grassland/Herbaceous
72	Sedge/Herbaceous
73	Lichens (Alaska Only)
74	Moss (Alaska Only)
81	Pasture/Hay
82	Cultivated Crops
90	Woody Wetlands
95	Emergent Wetlands

10	Water
21	Developed, Open Space
22	Developed, Low Intensity
23	Developed, Medium Intensity
24	Developed, High Intensity
30	Barren
40	Forest
50	Shrub
70	Herbaceous
80	Cultivated
90	Wetlands

3.2.3 Zonal Statistics: Spatial analyses of surface temperature by land cover class

Three tables of zonal statistics were developed in order to determine the relationship between land cover classes and the difference in surface temperatures between 1993-2011. The zonal statistics tool provides a summary of simple statistics based on groups. For this analysis, surface temperatures were summarized by NLCD classes. Output statistics included minimum, maximum, mean, standard deviation, range, area, and sum values. Temperatures were calculated for each and for all NLCD class.

4.0 RESULTS

4.1 Results of Objective 1: Have land surface temperatures (LST) increased in Austin, Texas between 1993 and 2011?

Maps of average temperatures and temperature difference are presented for 1993 (Figure 1), 2011 (Figure 2) and the difference between 1993 and 2011 (Figure 3).

Figure 1: Average LST for Austin, TX from July-August, 1993

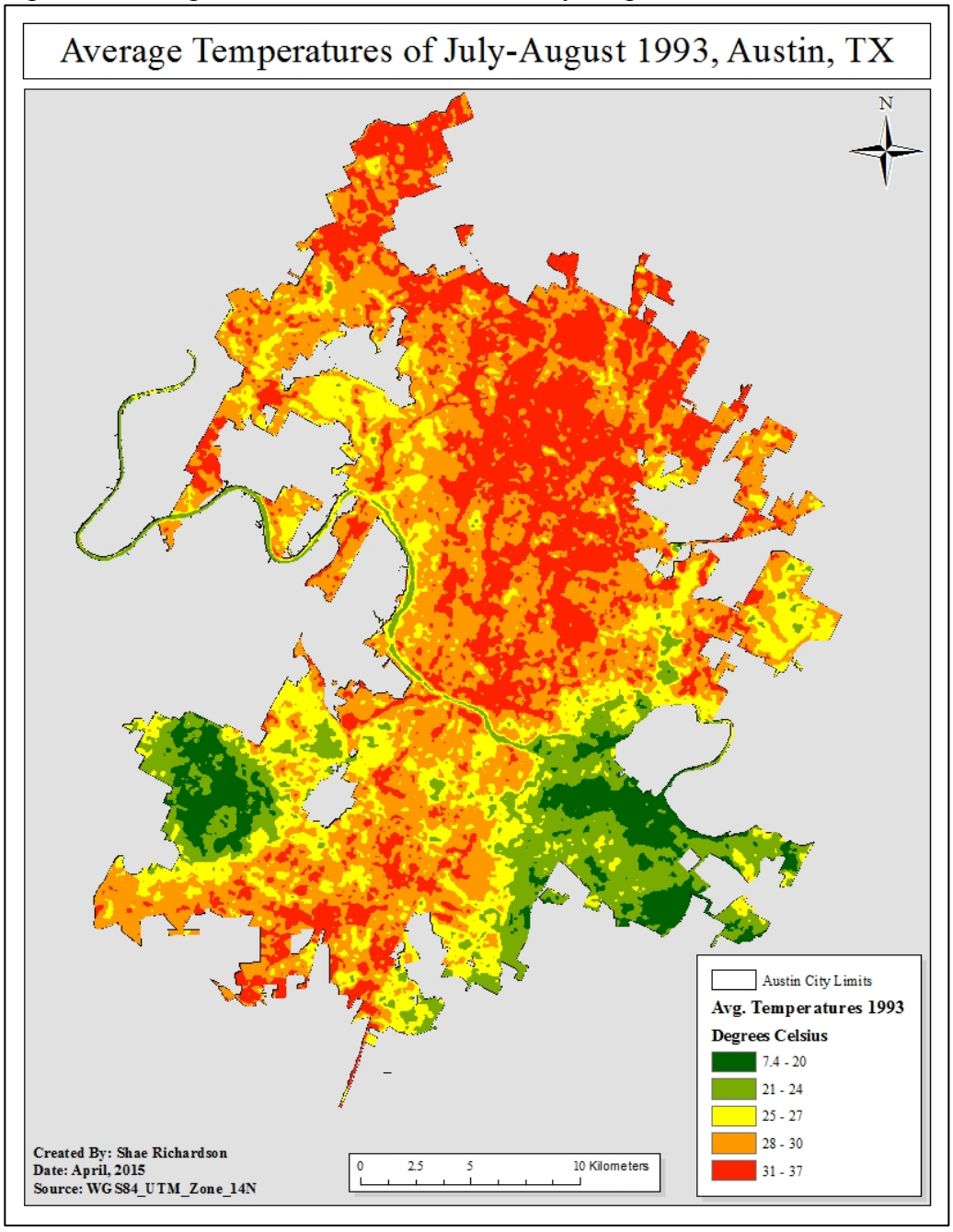

Figure 2: Average LST for Austin, TX from July-August, 2011

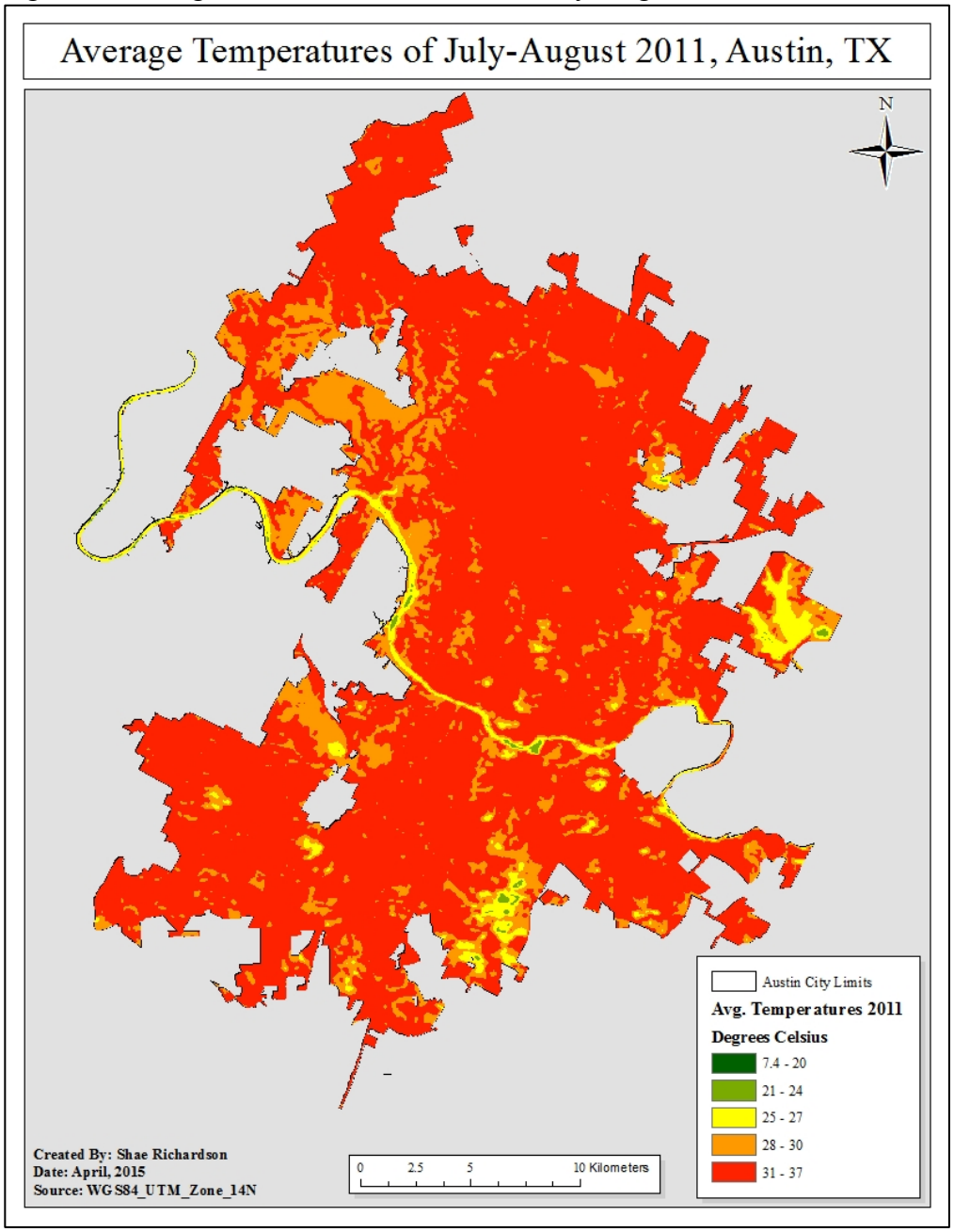

Figure 3: Austin's LST difference from 1993 to 2011

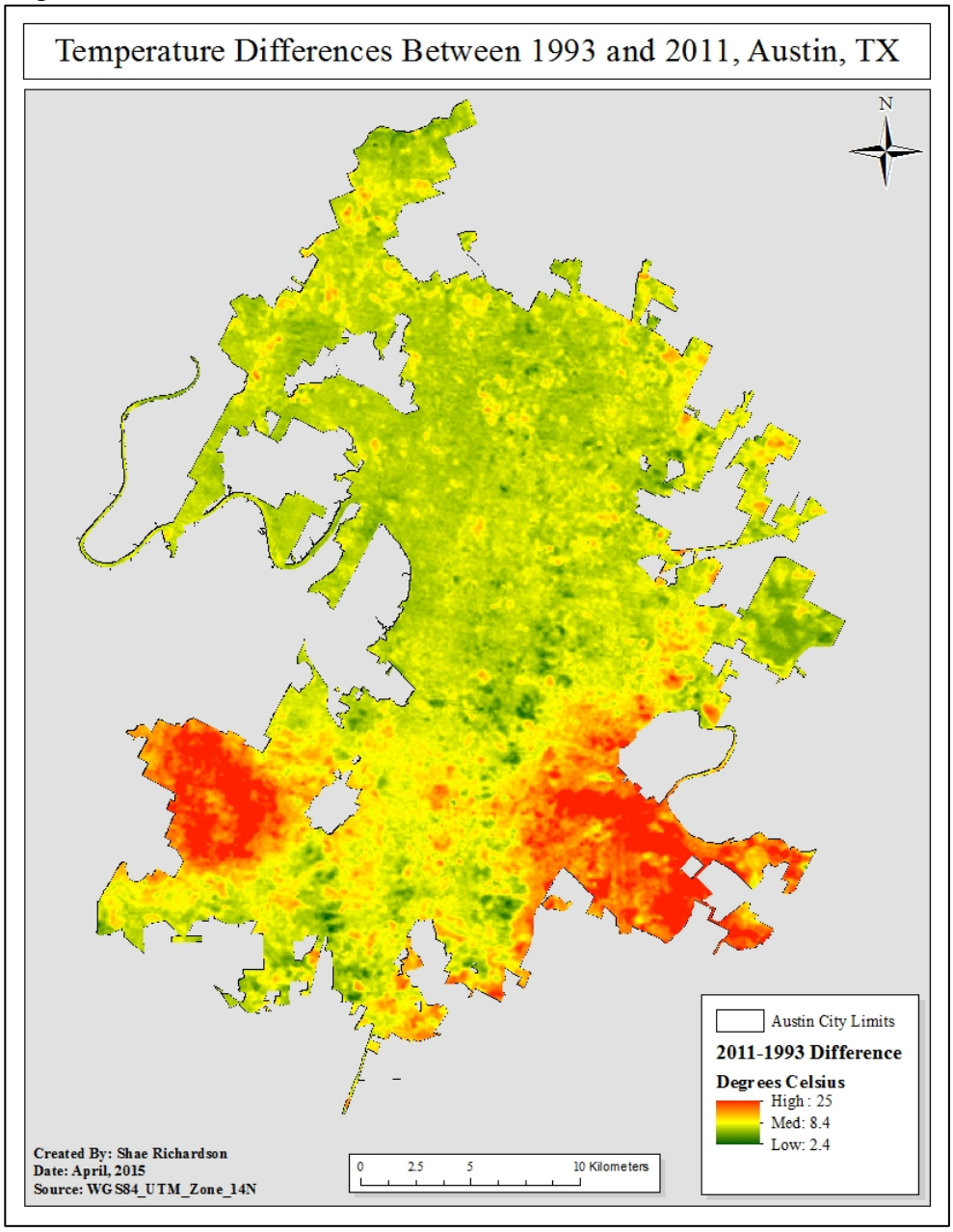

Based on the analysis, between 1993 to 2011, land surface temperatures increased by an average of 4.7 degrees C. In 2011, the majority of Austin's metropolitan area displays an average surface temperature of 31 degrees C or higher (temperature range of 7.4 degrees

C – 37.0 degrees C). While in 1993, areas of such temperatures are much more compact with the surrounding areas having a much wider range of surface temperatures (7.4 – 30 degrees C).

Figure 3 represents the change in average surface temperatures between 1993 and 2011. Results show the areas of the largest temperature changes are located in the southern half of the city.

4.2 Results of Objective 2: Does land cover type influence land surface temperatures?

Figures 4 and 5 represent the reclassified land cover types for the 1992 and 2011 NLCD classes.

Figure 4: Reclassified NLCD for 2011

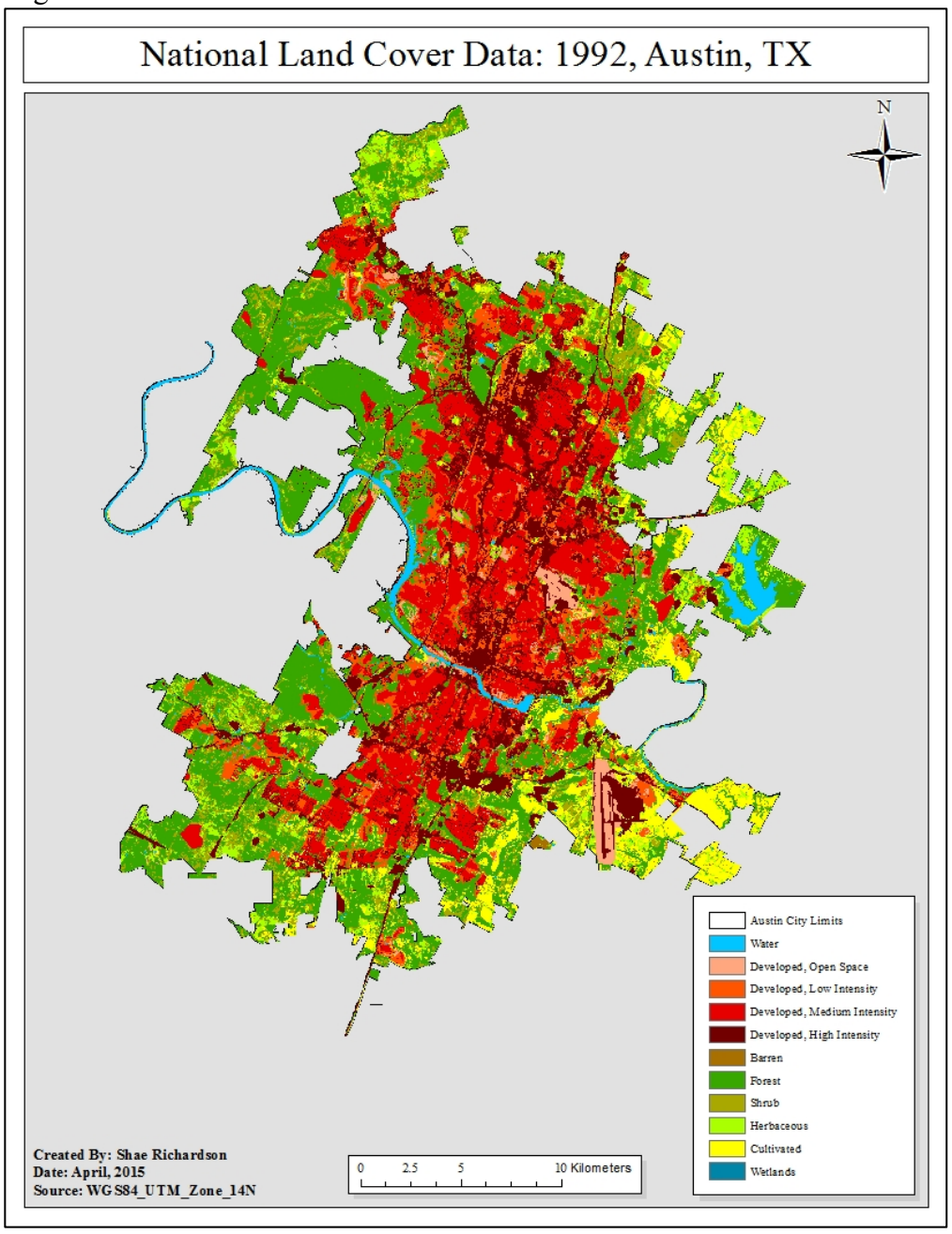

Figure 5: Reclassified NLCD for 2011

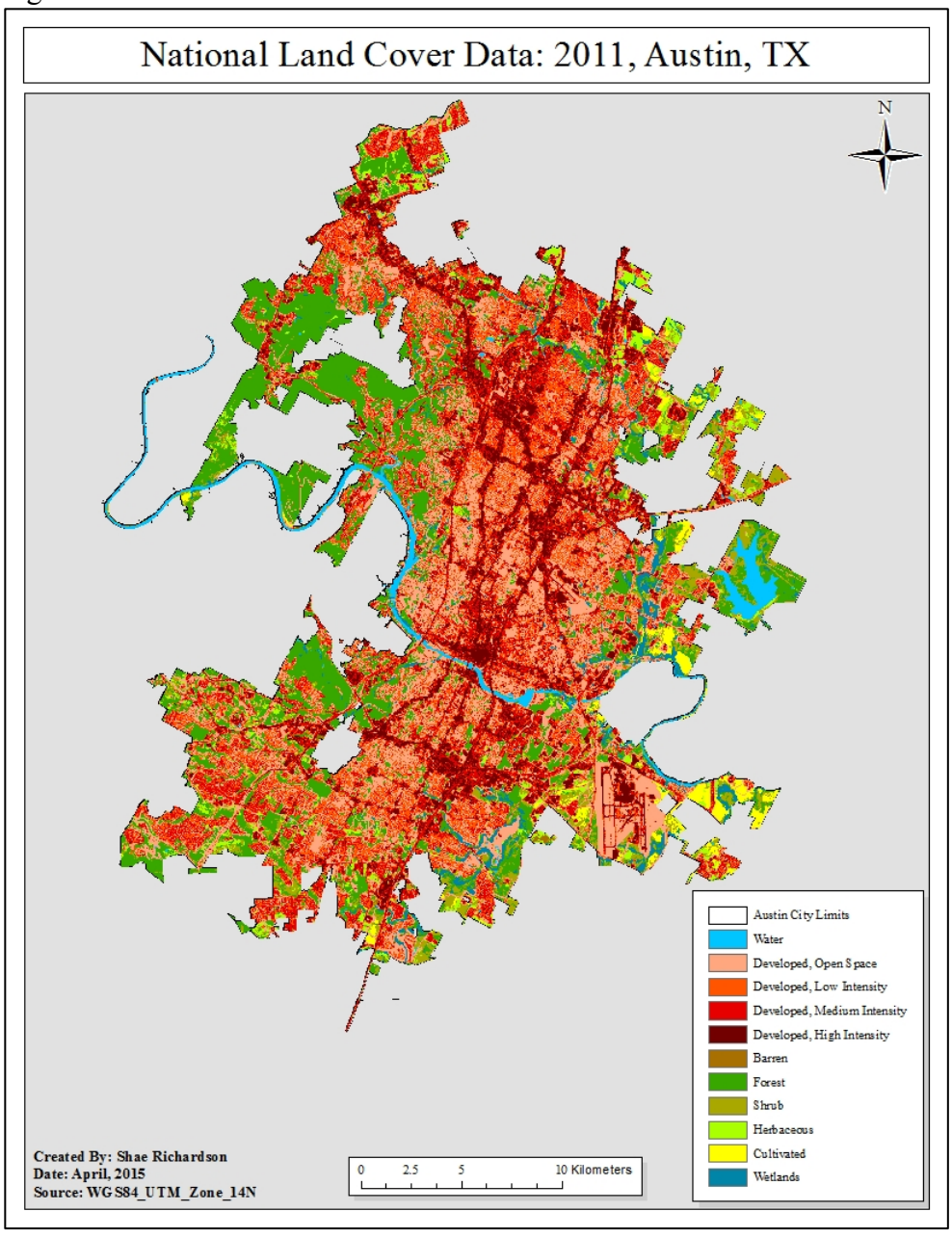

Based on the zonal statistics analysis, between 1993 and 2011 mean land surface temperatures for developed, medium intensity (DMI) increased by 4.20 degrees C. A

similar increase was observed for developed, low intensity (DLI) and developed, high intensity (DHI) (4.39 and 3.90 degrees C, respectively). A summary of land surface temperatures by land cover class and the difference between analysis years is provided in Table 5.

Zonal statistics for 1993 indicate that land surface temperatures associated with developed pixels have an average temperature of 27.9 degrees C, with the DHI resulting in the highest average temperature of 28.9 degrees C (standard deviation of 3.7 degrees C). The lowest average surface temperature was observed for the water class (23.8 degrees C, +/- 2.7 degrees C).

The average surface temperature for developed land in 2011 was 32.3 degrees C. The highest average temperatures, however, were associated with the cultivated land class ((33.5 degrees C, +/- 1.9 degrees C), while DHI is shown as the second highest at 32.9 degrees C (+/- 1.4 degrees C). The lowest surface temperatures correspond to the water class (25.5 degrees C, +/- 1.7 degrees C) and wetlands (28.8 degrees C, +/- 1.9 degrees C). However, the forested land cover also exhibited lower surfaces temperatures than the rest of the land classes (29.8 degrees C, +/- 1.7 degrees C).

The land cover that exhibited the largest change in temperature between 1993 and 2011 was the cultivated land class, with an average increase of 8.6 degrees C, although the cultivated class also has the highest standard deviation (4.2 degrees C), indicating a larger variation in average temperatures.

Table 5: Mean and standard deviation of surface temperatures by land cover class

Year	**1993 Avg. Temp (°C)**		**2011 Avg. Temp. (°C)**		**2011; Change in LST (°C)**	
NLCD: Class Name	**Mean**	**Std. Dev.**	**Mean**	**Std. Dev.**	**Mean**	**Std. Dev.**
Water	23.8	2.7	25.5	1.7	1.9	2.2
Developed, Open Space	26.7	4.3	31.7	1.8	4.6	3.9
Developed, Low Intensity	27.7	3.5	32.1	1.5	4.1	3.5
Developed, Medium Intensity	28.6	2.4	32.5	1.5	4.2	3.6
Developed, High Intensity	28.9	3.7	32.9	1.4	3.9	3.5
Barren	25.3	4.6	31.8	2.1	6.2	3.9
Forest	26.1	3.2	29.8	1.7	3.6	3.1
Shrub	27.4	3.9	31.6	2.1	5.4	3.9
Herbaceous	27.9	3.8	32.9	1.9	5.0	3.8
Cultivated	25.4	4.4	33.5	1.9	8.6	4.2
Wetlands	25.6	3.4	28.8	1.9	4.5	3.3

5.0 DISCUSSION

5.1 Influence of increased development between 1993-2011

The influence of increased development and correspondence with the increase in surface temperatures indicates the presence of the urban heat island effect. Average surface temperatures, by analysis of land cover class indicated in that general, developed areas had higher surface temperatures compared to most undeveloped areas. However, the largest surface temperature increases were found for areas outside of the developed classes. The barren and cultivated classes showed the greatest increase, which can be attributed to a variety of factors including urban encroachment in 2011.

The increased surface temperatures of the developed areas are not geographically static and may spread out and have a significant influence on the areas of which they are moving into or the areas that directly border them. Another considerable factor may be that the areas of cultivated (planted) land in 1992 could have been more densely planted with little bare soil in between. While the cultivated class in 2011, due to heavy drought influence, it is possible that fewer plants were present and therefore an increase of drier, bare soils, which will absorb more incident energy. Barren land is classified by NLCD as areas of little to no vegetation such as, rock, sand, and clay. These types of materials are similar to materials used in development (concrete) and exhibit less-evaporative and less-transpiring properties. Thus, higher temperatures are to be expected for barren land areas. As the amount of heat stored in the soil and surface structures is much higher than the amount of heat stored in more densely vegetated areas.

5.2 Potential sources of error and uncertainty

Potential uncertainties in surface temperatures may be attributed to the limited number of Landsat images used in this analysis. Though the analysis may have benefited from the averaging of more Landsat images, the results still show a significant temperature increase and enable the presence of SUHI to be detected. As previously stated, 2011 experienced drought conditions that year, which may have an impact on increased surface temperatures, especially in the areas of barren and fallow land, due to decrease evaporation of moisture from the soil. Different classification schemes may also have an influence of possible uncertainties for this analysis. Digital image pixels are frequently misclassified and those errors will propagate throughout an analysis.

6.0 CONCLUSION

In conclusion, the methods presented in this analysis indicate the urban heat island effect is present between 1992 and 2011 for Austin, Texas. The methods used in this analysis can serve as a suitable framework for determining surface temperatures and how they correspond with land cover classes. These methods should be transferrable to another city for which Landsat and NLCD data are available. This analysis could be used to investigate strategies that would help to mitigate UHI effects and help determine which methods are possible for large communities to implement and where they would be most beneficial. Lastly, this analysis would be beneficial to perform in the future to continue monitoring how surface temperatures change in urban environments.

REFERENCES

Carlyle, E (2014). *Americas 20 Fastest Growing Cities*. Forbes, Retrieved From http://www.forbes.com/sites/erincarlyle/2014/02/14/americas-20-fastest-growing-cities/

Centers For Disease Control and Prevention. (July, 2009) *Extreme Heat Prevention Guide.* Retrieved From http://emergency.cdc.gov/disasters/extremeheat/heat_guide.asp

City Of Dallas Urban Forest. (March, 2015) *Addressing Dallas' Urban Heat Island Effect.* Retrieved From http://dallastrees.org/?page_id=104

Graham, S. (September, 1999). *Remote Sensing: Introduction and History*. NASA Earth Observatory. Retrieved From http://earthobservatory.nasa.gov/Features/RemoteSensing/

Jensen, John R. (2007). *Remote Sensing of the Environment: An Earth Resource Perspective 2nd Ed.* Upper Saddle River, NJ: Pearson Education, Inc.

Mallick, J., Kant, Y., Bharath, B.D. (2008). Estimation of land surface temperature over Delhi using Landsat-7 ETM+. *J. Ind. Geophys. Union 12*(3), 131-140.

NASA, Landsat Science. (April, 2015). *The Landsat Program.* Retrieved From http://landsat.gsfc.nasa.gov

Oke, T.R. (1976). The distinction between canopy and boundary-layer urban heat islands. *Atmosphere 14*, 268-277.

Quattrochi, D.A., Lo, C.P., Luvall, J.C., (1996). Application of high-resolution thermal Infrared remote sensing and GIS to assess the urban heat island effect. *Int. J. Remote Sensing, 18*(2), 287-304.

Realty Austin. (2015). Reasons to Live in Austin, TX. Retrieved From https://www.realtyaustin.com/relocation/reasons-to-live-in-austin.php

Robison, R. (2015). *Austin Area Population Histories and Forecasts*. City of Austin. Retrieved From http://www.austintexas.gov/sites/default/files/files/Planning/Demographics/austin_forecast_2015_annual_pub.pdf

Roth, M., Oke, T.R., Emery, W.J. (1989). Satellite-derived urban heat islands from 3 coastal cities and the utilization of such data in urban climatology. *International Journal of Remote Sensing 10*(11), 1699-1720.

Stathopoulou, M., Cartalis, C. (2007) Daytime urban heat islands from Landsat ETM+ and Corine Land Cover data: An application to major cities in Greece. *Solar Energy 81,* 358-368.

UCAR, Center for Science Education. (2011). *Urban Heat Islands.* Retrieved From http://scied.ucar.edu/longcontent/urban-heat-islands

United States Evironmental Protection Agency. (August, 2013). *Heat Island Impacts.* Retrieved From http://www.epa.gov/hiri/impacts/index.htm

United States Evironmental Protection Agency. (2005). *Cool Pavements Compendium: Reducing UHI* [PDF]. Retrieved From http://www.epa.gov/heatislands/resources/pdf/CoolPavesCompendium.pdf

Vega, A.J., Rohli, R.V. (2012). *Climatology 2nd Ed.* Sudbury, MA: Jones & Barlett Learning.

Voogt, J.A., Oke, T.R. (2003). Thermal remote sensing of Urban Climates. *Remote Sensing of Environment 86*(3), 370-384.

Wade, T., Sommer, S. (2006). *A to Z GIS: An illustrated dictionary of geographic information systems*. Redlands, CA: ESRI Press.

Zhang, P., Wolfe, R.E., Imoff, M.L., Bounoua, L. (2009). Remote Sensing of the urban heat island effect across biomes in the continental USA. *Remote Sensing of Environment 114,* 504-513.